Supplemental Table and Figures

	CaMKII	PV	VIP	SST
MGv	✓	✓	✓	✓
MGd	✓	✓	✓	✓
SGN	✓	✓	✓	✓
MGm	✓	✓	✓	✓
POL	✓	✓		✓
ZI	✓	✓	✓	✓
SIn	✓	✓	✓	✓
HY	✓	✓		✓
LA	✓	✓		✓
AUDd	✓	✓	✓	✓
AUDv	✓	✓	✓	✓
PTLp	✓	✓		✓
SS	✓	✓	✓	✓
RSP	✓	✓		✓
VIS	✓	✓		✓
OFC	✓	✓		✓
M1	✓	✓		✓
M2	✓	✓	✓	✓
Cg	✓	✓		
CLA	✓	✓	✓	✓

Table S1 – refers to Figure 1. Afferents to ACtx Cell Types

Brain regions with GFP^+ neurons providing input to $CaMKII^+$, PV^+, SST^+, or VIP^+ neurons. Blue colors indicate thalamic regions; orange colors indicate subthalamic regions; grey colors indicate cortical regions. Abbreviations of brain regions: medial geniculate body, ventral part (MGv), medial geniculate body, dorsal part (MGd), suprageniculate nucleus (SGN), medial geniculate body, medial part (MGm), posterior limiting nucleus of the thalamus (POL), zona incerta (ZI), substantia innominata (SIn), hypothalamus (HY), lateral amygdala (LA), auditory cortex, dorsal part (AUDd), auditory cortex, ventral part (AUDv), posterior parietal association areas (PTLp), somatosensory cortex (SS), retrosplenial cortex (RSP), visual cortex (VIS), orbitofrontal cortex (OFC), primary motor cortex (M1), secondary motor cortex (M2), cingulate cortex (Cg), claustrum (CLA).

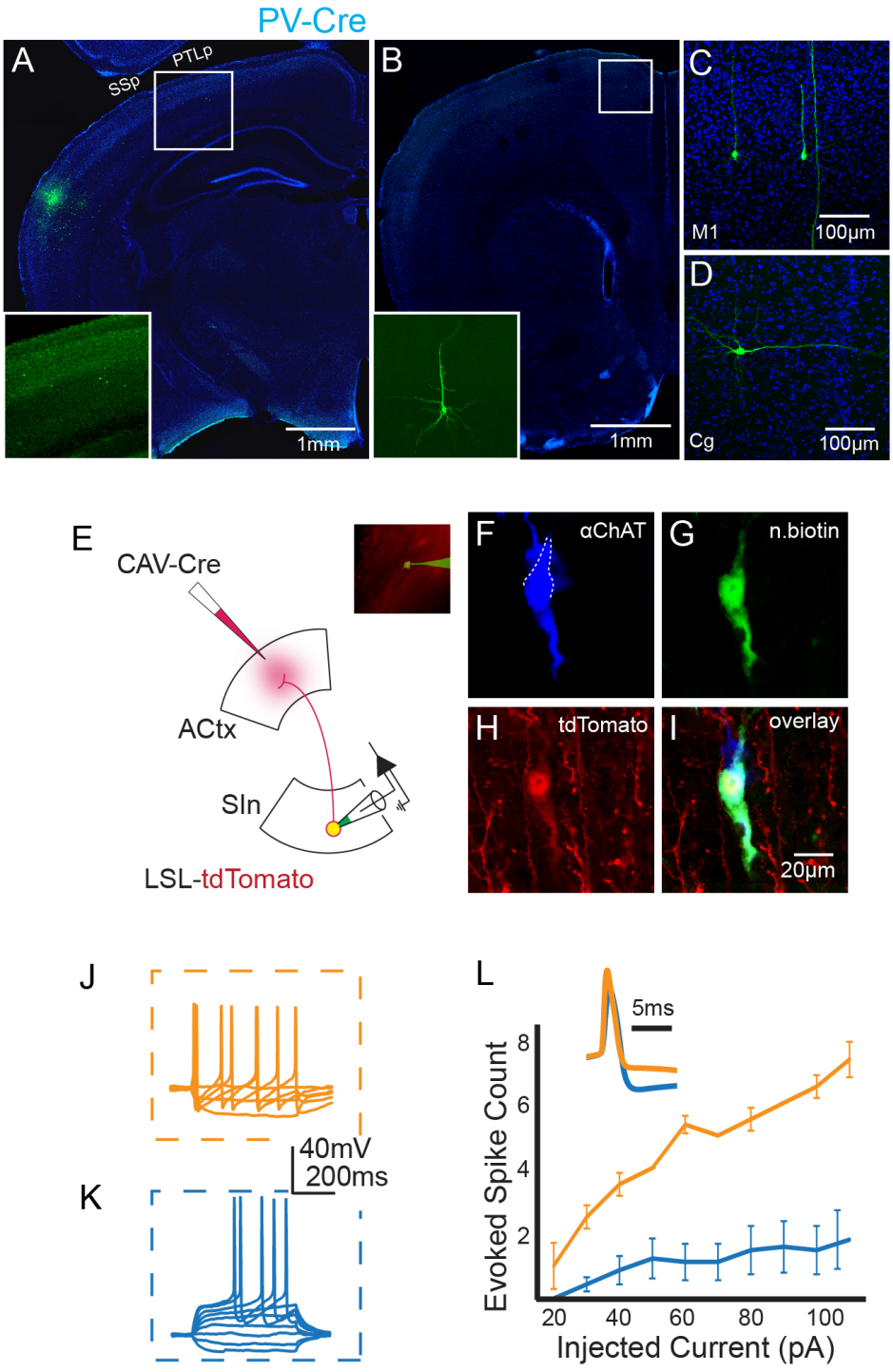

Figure S1 – refers to Figure 1. Afferents to ACtx Cell Types and Electrophysiological Properties of SIn_{ACh} Neurons

(A) Neurons presynaptic to auditory cortical PV^+ neurons. The boxed region corresponds to the inset, depicting neuronal labeling near SS and PTLp. The inset is shown without DAPI staining for clarity. (B) GFP^+ neuron in M2. The boxed region corresponds to the inset. (C) GFP^+ neurons in M1. (D) GFP^+ neurons in Cg. (E) Strategy for recording from SIn_{ACh} neurons. CAV-Cre was injected into ACtx of Ai14

mice, resulting in tdTomato labeling of its afferents. Whole-cell recordings were made from tdTomato$^+$ neurons in SIn (inset). (F-I) Following whole-cell recording, sections were immunostained for ChAT (F), and targeted tdTomato$^+$ neurons were visualized (G,H), confirming their cholinergic phenotype (I). (J-L) Neurons fell into one of two electrophysiological classes: "early spiking" neurons (J) or "late spiking" neurons (K)(Unal et al., 2010). These classes additionally segregated by their action potential responses to intracellular current injection (L), as well as action potential shape (inset).

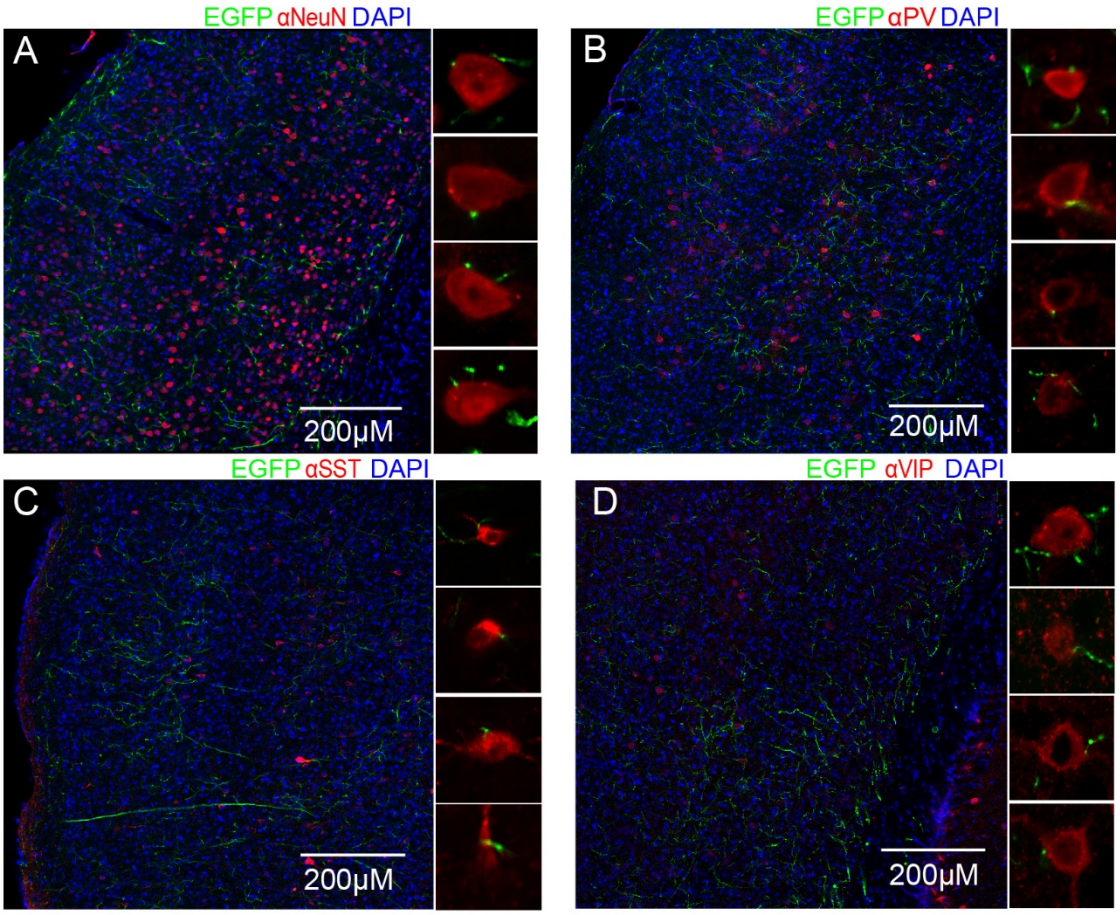

Figure S2 – refers to Figure 1. SIn_{ACh} Neurons Form Close Appositions with Neurons in ACtx

(A) SIn_{ACh} axons in ACtx, made to express GFP by injecting AAV-FLEX-GFP into SIn of ChAT-Cre mice. In red are neurons immunostained for NeuN. The panels to the right show close appositions between GFP$^+$ SIn_{ACh} axons and NeuN$^+$ neurons. Images are single optical sections of 1 or fewer AU taken with a 100x 1.4 NA oil immersion objective. DAPI is blue. (B-D) GFP$^+$ SIn_{ACh} axons form close appositions with cell bodies and dendrites of PV$^+$, SST$^+$, and VIP$^+$ neurons in ACtx.

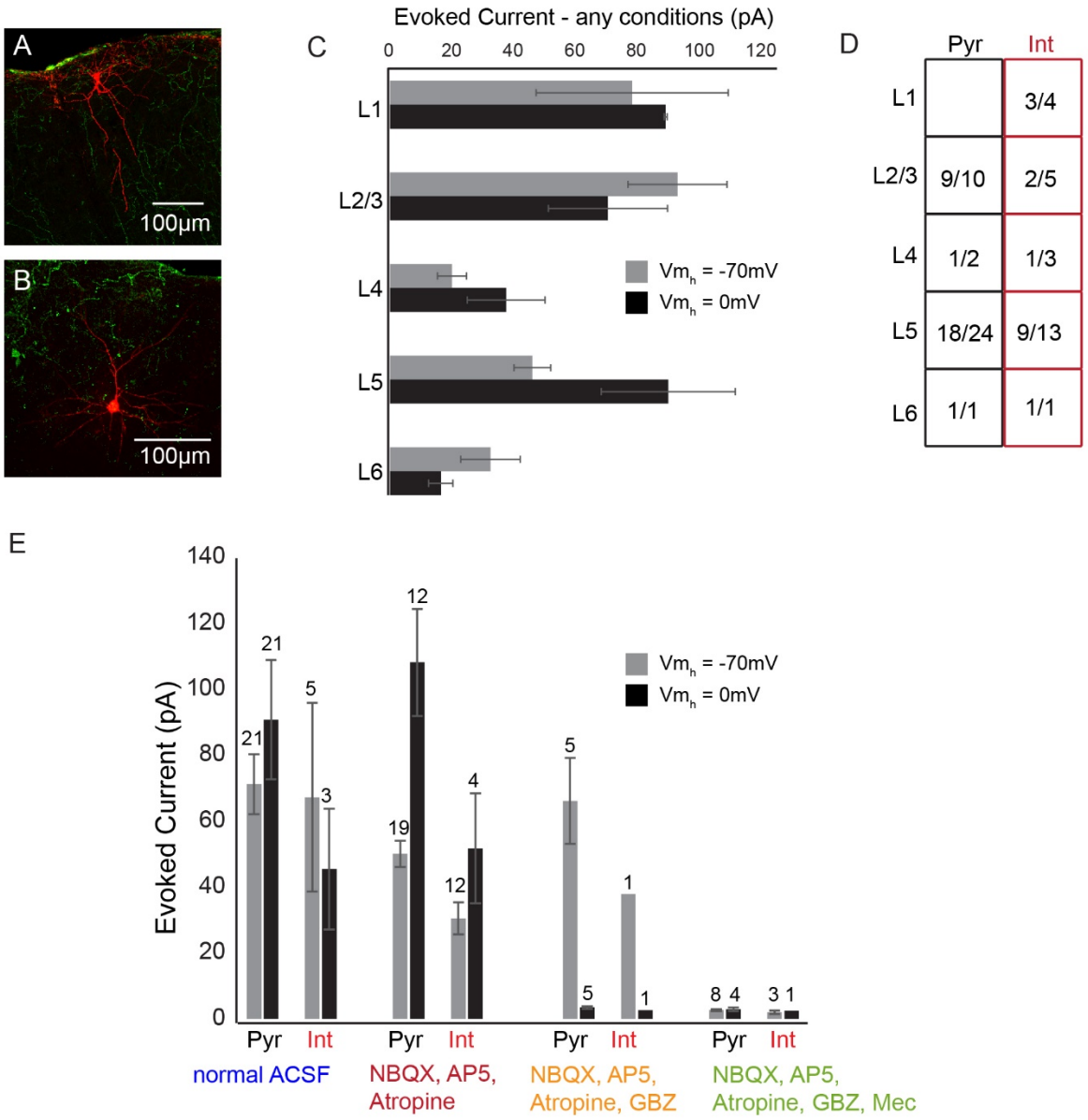

Figure S3 – refers to Figure 2. Excitatory and Inhibitory Currents in ACtx Mediated by Stimulation of SIn_{ACh} axons.

(A) A confocal micrograph of a L1 interneuron filled with dye and visualized following whole-cell recording. SIn_{ACh} axons expressing ChR2 and GFP (antibody enhanced fluorescence) are in green. (B) A confocal micrograph of a L2/3 pyramidal neuron filled with dye and visualized following whole-cell recording. (C) Average excitatory (holding potential at -70 mV) and inhibitory (holding potential at 0 mV) currents evoked in neurons across all layers of ACtx. (D) The fraction of pyramidal neurons (black squares) or interneurons (red squares) responsive to stimulation of SIn_{ACh} axons, recorded from across layers. (E) The same data from Figure 2I, separated into pyramidal neurons and interneurons. The numbers of cells recorded for each condition are indicated above the bars. Values are mean ± SEM.

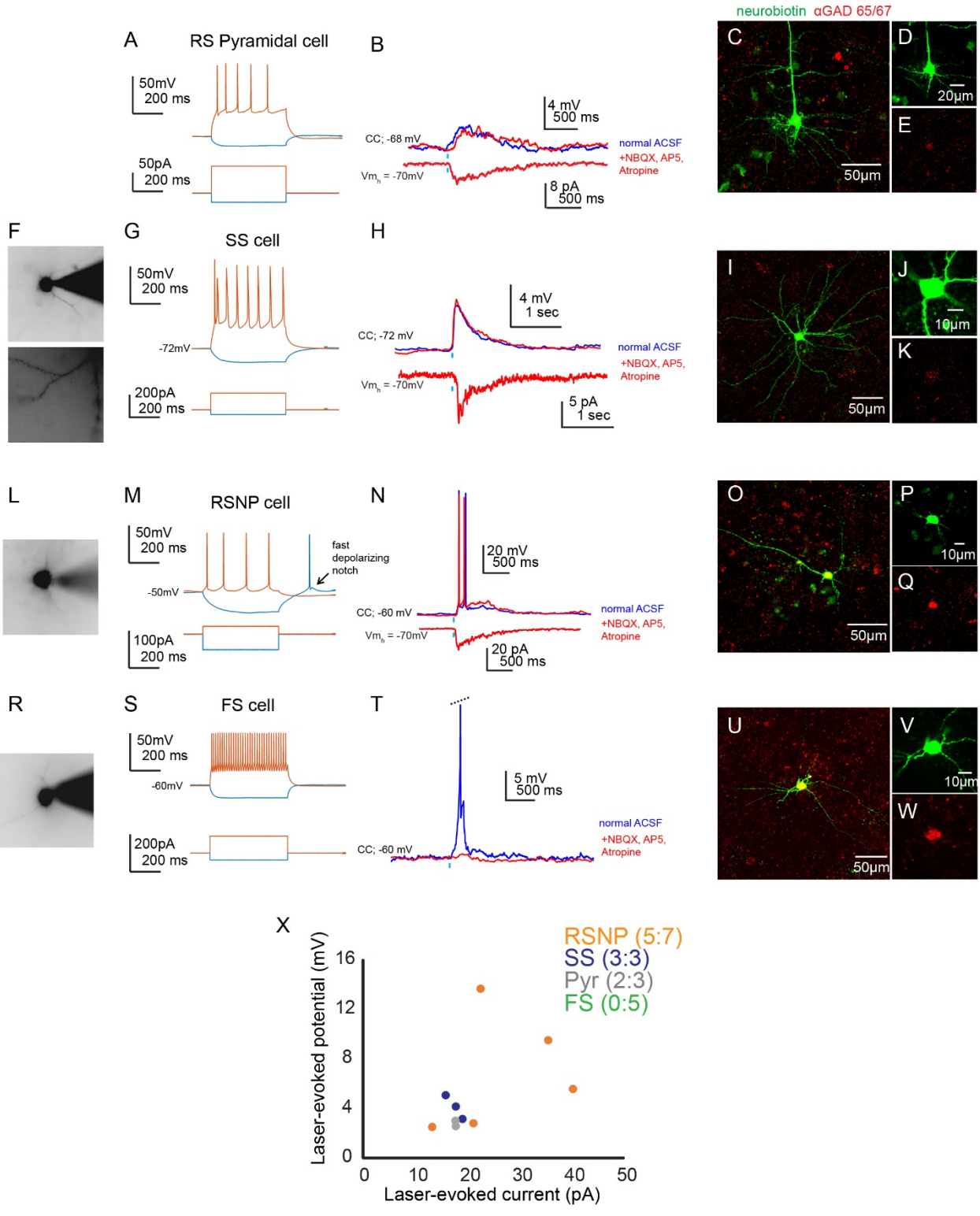
neurobiotin αGAD 65/67
A
RS Pyramidal cell
50mV
200 ms
50pA
200 ms
B
4 mV
500 ms
CC; -68 mV
Vm_h = -70mV
normal ACSF
+NBQX, AP5,
Atropine
8 pA
500 ms
C
D
20μm
E
50μm
F
G
SS cell
50mV
200 ms
-72mV
200pA
200 ms
H
4 mV
1 sec
CC; -72 mV
Vm_h = -70mV
normal ACSF
+NBQX, AP5,
Atropine
5 pA
1 sec
I
J
10μm
K
50μm
L
M
RSNP cell
50mV
200 ms
fast
depolarizing
notch
-50mV
100pA
200 ms
N
20 mV
500 ms
CC; -60 mV
Vm_h = -70mV
normal ACSF
+NBQX, AP5,
Atropine
20 pA
500 ms
O
P
10μm
Q
50μm
R
S
FS cell
50mV
200 ms
-60mV
200pA
200 ms
T
5 mV
500 ms
CC; -60 mV
normal ACSF
+NBQX, AP5,
Atropine
U
V
10μm
W
50μm
X
RSNP (5:7)
SS (3:3)
Pyr (2:3)
FS (0:5)
Laser-evoked potential (mV)
0
4
8
12
16
0
10
20
30
40
50
Laser-evoked current (pA)

66

Figure S4 – refers to Figure 2. Recording SIn_{ACh}-Evoked Activity in Identified Inhibitory and Excitatory Interneurons.

(A) Membrane properties (above) of a pyramidal cell revealed by intracellular current injection (below). (B) Responses to SIn_{ACh} stimulation in current clamp configuration (above, resting membrane potential indicated) and in voltage clamp configuration (below, holding potential indicated). Recordings were made in nACSF (blue traces) and ACSF containing NBQX, AP5, and atropine (red traces). (C) Confocal Z stack depicting a pyramidal cell targeted for whole cell physiology (green) and GAD65/67 labeling (red). (D,E) Single optical sections of the green and red channels from (C). Note the absence of substantial GAD immunolabeling in (E). (F) A spiny stellate cell filled with fluorescent dye during whole cell recording (above), and a higher magnification view of spiny dendrites from the same cell (below). (G) Membrane properties of a spiny stellate cell revealed by intracellular current injection. (H) Responses of a spiny stellate cell to SIn_{ACh} stimulation. (I) Confocal Z stack depicting a spiny stellate cell targeted for whole cell physiology (green) and GAD65/67 labeling (red). (J,K) Single optical sections of the green and red channels from (I). Note the absence of substantial GAD immunolabeling in (K). (L) A regular spiking nonpyramidal (RSNP) cell filled with fluorescent dye during whole cell recording. (M) Membrane properties of a RSNP cell revealed by intracellular current injection. Note the fast depolarizing notch following an action potential induced by cessation of the hyperpolarizing current pulse. (N) Responses of a RSNP cell to SIn_{ACh} stimulation. (O) Confocal Z stack depicting a RSNP cell targeted for whole cell physiology (green) and GAD65/67 labeling (red). (P,Q) Single optical sections of the green and red channels from (O). Note the substantial GAD immunolabeling in (Q) colocalizing with the targeted neuron. (R) A fast spiking (FS) cell filled with fluorescent dye during whole cell recording. (S) Membrane properties of FS cell revealed by intracellular current injection. (T) Responses of a FS cell to SIn_{ACh} stimulation. Voltage responses evoked in nACSF were abolished upon application of NBQX, AP5, and atropine. (U) Confocal Z stack depicting a FS cell targeted for whole cell physiology (green) and GAD65/67 labeling (red). (V,W) Single optical sections of the green and red channels from (U). Note the substantial GAD immunolabeling in (W) colocalizing with the targeted neuron. (X) Laser-evoked excitatory current plotted against laser-evoked depolarizing potential for each responsive neuron, color coded by neuron type. The inset indicates the cell type, as well as the number of responsive neurons out of the total number recorded for each cell type.

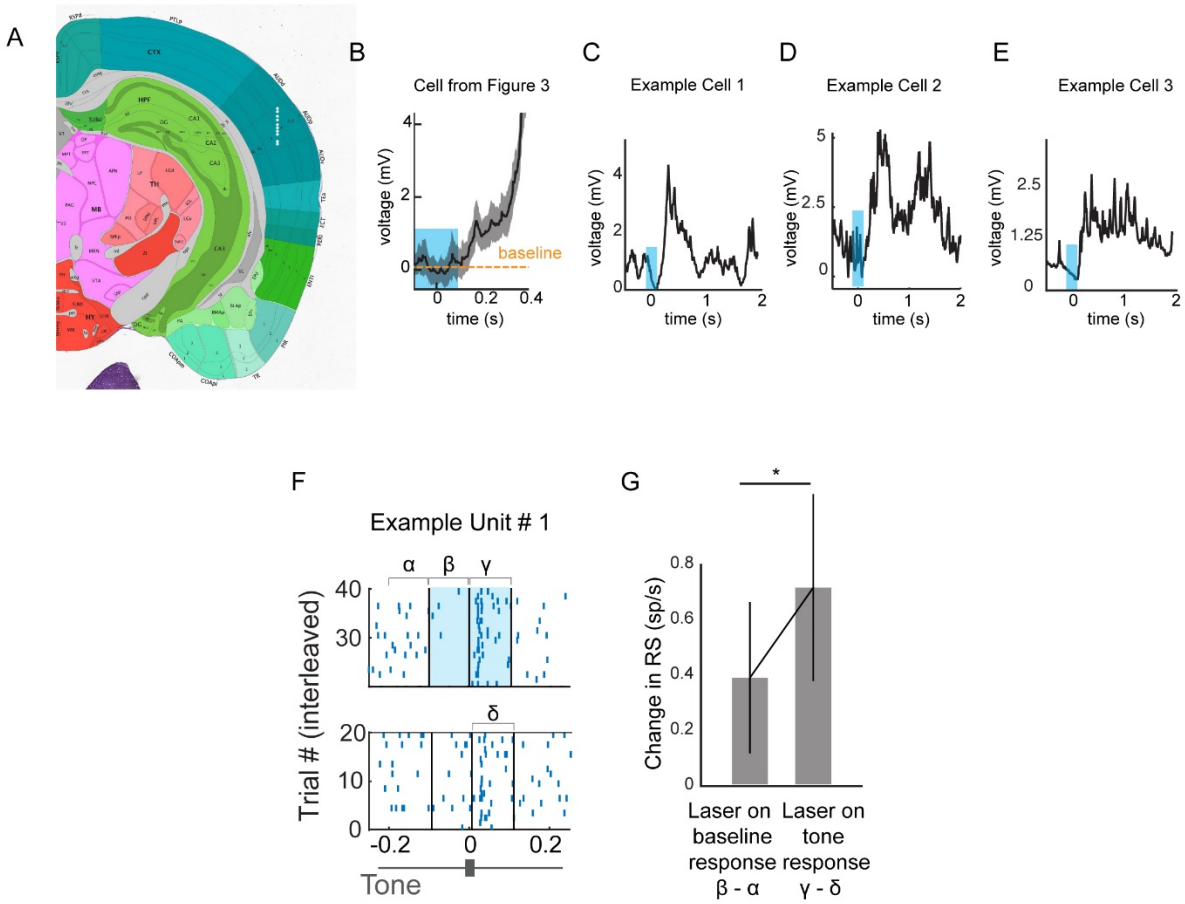

Figure S5 – refers to Figures 3 and 4.

(A) Representative coronal section from the Allen Brain Atlas with approximate locations of intracellularly-recorded neurons included in Figure 3. Recorded neurons spanned superficial and deep layers. (B) An expanded view of the exemplar neuron in Figure 3, depicting the depolarization following optogenetic stimulation of SIn_{ACh} axons. The mean membrane potential of the baseline period is indicated. (C-E) Three additional example neurons' responses to optogenetic stimulation of SIn_{ACh} axons, which are included in Figure 3. (F) The strategy for determining the relative modulation of baseline firing rate versus tone-evoked firing rate in response to optogenetic stimulation of SIn_{ACh} axons. (G) The change in response strength following optogenetic stimulation of SIn_{ACh} axons for baseline and for tone-evoked responses. (*$p < 0.05$, paired t-test). Values are mean ± SEM.

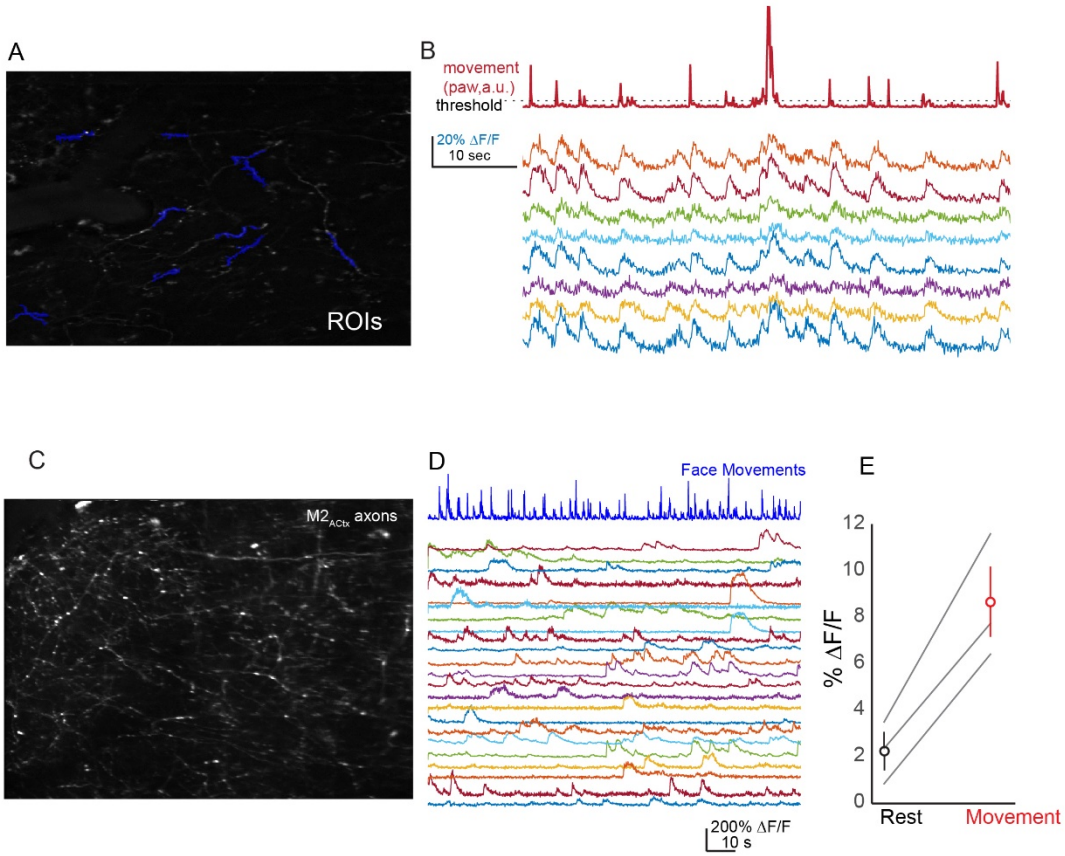

Figure S6 – refers to Figure 5. Two Photon Calcium Imaging of SIn_{ACh} and $M2_{ACtx}$ Axons

(A) An average intensity projection of an example field of view from 2p imaging of SIn_{ACh} axons in ACtx, with axon segment ROIs marked with blue shading. (B) Activity of several SIn_{ACh} axon ROIs in a 2p imaging field of view (multicolored traces below) during an epoch of small movements (above red trace). The threshold for movement is indicated by the dashed line. (C) An average intensity projection of an example field of view from 2p imaging of $M2_{ACtx}$ axons. (D) Activity of several $M2_{ACtx}$ axon ROIs in a 2p imaging field of view (multicolored traces below) during an epoch of small movements (above blue trace). (E) ΔF/F of $M2_{ACtx}$ axons during periods of rest and movement.

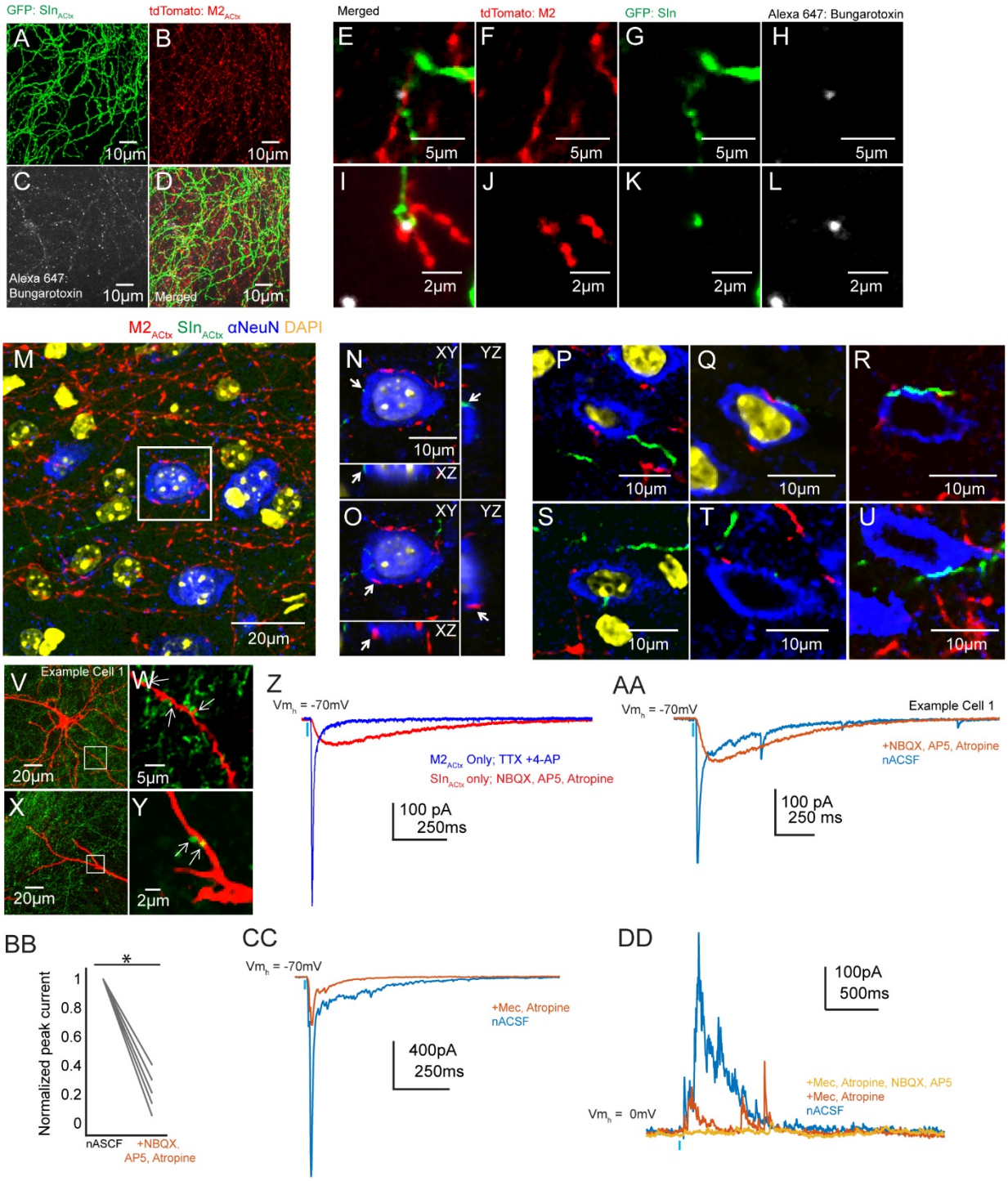

Figure S7 – refers to Figure 7. SIn$_{ACh}$ and M2$_{ACtx}$ Synapses Converge on Single Auditory Cortical Neurons

(A-D) Single fluorescence channels of the same data from Figure 7E. Bungarotoxin Alexa Fluor 647 fluorescence brightness is increased in (C) to highlight the density of labeled nicotinic acetylcholine receptors. (E-L) Single optical sections depicting close appositions (potential presynaptic contacts)

between M2 and SIn_{ACh} axons in ACtx. The channel colors indicate the same information as in (A-D). (M) A confocal Z stack of neurons labeled with NeuN (blue) in the vicinity of SIn_{ACh} axons (green) and $M2_{ACtx}$ axons (red). DAPI is yellow. (N,O) Single optical sections of the boxed cell from (M). Close appositions are indicated with arrows. The images labeled YZ and XZ are the orthogonal planes of those appositions depicted in the XY planes. (P-U) Six more single optical sections of additional cell bodies labeled with NeuN showing close appositions with M2 and SIn_{ACh} axons. No DAPI was used in (R), (T), or (U). (V-Y) Confocal Z stacks (V,X) and single optical sections (W,Y) showing close appositions between putative ChR2-expressing M2 and SIn_{ACh} boutons and the dendrites of a pyramidal neuron targeted for whole cell recording. Same cell as in Figure 7J. (Z) An example monosynaptic (ACSF containing TTX and 4-AP) glutamatergic excitatory current (blue) evoked by stimulation of only $M2_{ACtx}$ axons expressing ChR2 (data from Nelson et al. 2013). An example nicotinic (in NBQX, AP5, and atropine) excitatory current (red) evoked by stimulation of only SIn_{ACh} axons expressing ChR2 (data from Figure 2). The two traces are aligned at stimulus onset. (AA) A single cell example from experiments in Figure 7K. (BB) Normalized peak current evoked following stimulation of SIn_{ACh} and $M2_{ACtx}$ axons in nACSF and NBQX, AP5, and atropine. Peak excitatory current normalized to nACSF responses: 0.2263 ± 0.0643, $p = 2.73 \times 10^{-4}$ (CC) An example cell from experiments similar to those in Figure 7I-L, showing excitatory currents evoked following stimulation of SIn_{ACh} and $M2_{ACtx}$ axons, before (blue) and after (orange) addition of cholinergic transmission blockers. (DD) Same as (CC), but at holding potentials of 0mV to isolate inhibitory currents. ACSF with the addition of NBQX and AP5 was finally included to block all evoked inhibitory currents (yellow trace).

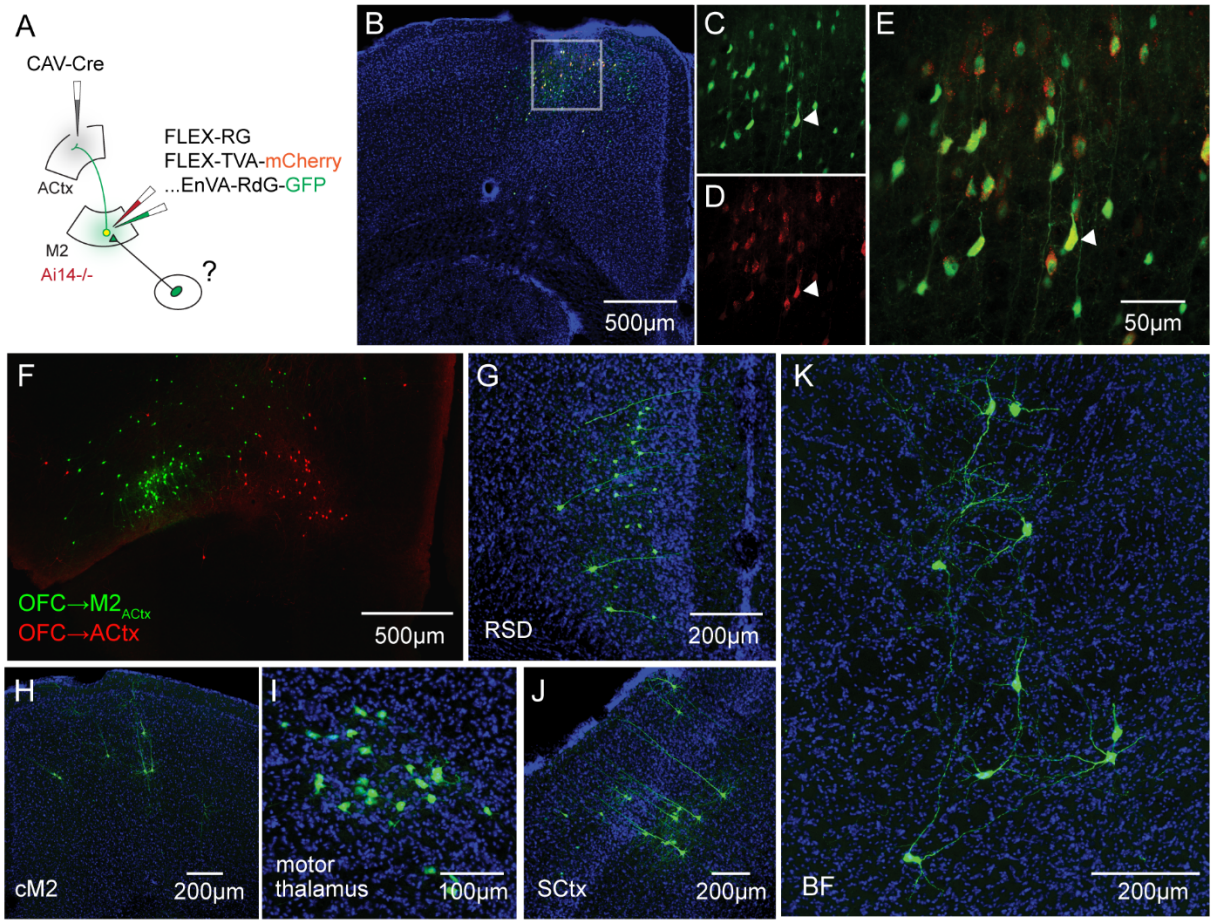

Figure S8 – refers to Figure 8. Synaptic Inputs to $M2_{ACtx}$ Neurons

(A) Schematic of the experimental strategy. On day 0, AAV-FLEX-RG and AAV-FLEX-TVA.mCherry were injected into M2 of wild type mice. Additionally, CAV-Cre was injected into ipsilateral ACtx. For a subset of mice, injections were made into Ai14 mice, which resulted in tdTomato labeling of afferents of ACtx. On Day 14, EnVA-RΔG.GFP is injected into M2, which labeled neurons presynaptic to $M2_{ACtx}$ cells expressing TVA and RG. (B) GFP and mCherry labeling in M2. DAPI is blue. (C) GFP^+ neurons from region outlined in (B). (D) $mCherry^+$ neurons in the same region. (E) An overlay of (C) and (D). The arrowhead indicates one of many $GFP^+mCherry^+$ starter neurons. (F) Neurons presynaptic to $M2_{ACtx}$ neurons (green) and neurons presynaptic to ACtx (red) in orbitofrontal cortex. These two classes of projection neurons are largely non-overlapping. (G-K) Neurons presynaptic to $M2_{ACtx}$ neurons in retrosplenial cortex (G), contralateral M2 (H), motor thalamus (I), somatosensory cortex (J), and rostral basal forebrain (K).

Supplemental Experimental Procedures

Animals

All experimental protocols were approved by Duke University Institutional Animal Care and Use Committee. Male and female wild-type (C57BL/6) and transgenic (PV-Cre, CaMKII-Cre, SST-Cre, VIP-Cre, ChAT-Cre, and Ai14) mice were purchased from Jackson Laboratories and housed and bred in an onsite vivarium. Mice selected for surgical and experimental procedures were kept on a reverse light cycle.

Stereotaxic Viral Injections

Mice aged 1-2 months (for in vitro electrophysiology) or 2-4 months (all other injections) were anesthetized with isoflurane (1-2% in O_2) and placed in a stereotaxic holder (Leica). A midline incision was made to expose the skull, and a craniotomy was made over the injection site. For rabies-based presynaptic tracing from ACtx, a pipette backfilled with an equal mixture of AAV.1.CAG.FLEX.RG (UNC Vector Core) and AAV.1.EF1α.FLEX.TVA-mCherry (UNC Vector Core) was angled 30 degrees from vertical and lowered into the brain. Approximately 150-300 nL of the mixture was pressure-injected into the center of ACtx over the course of 15 min. For anterograde tracing experiments, 300-400 nL of AAV.2/1.syn.FLEX.EGFP (Penn Vector Core) was injected into SIn, and 10-20 nL AAV.2/1.CAG.tdTomato (Penn Vector Core) was injected into the center of M2. For electrophysiological experiments, approximately 500-700 nL of AAV.2/1.EF1α.DIO.ChR2.GFP (Penn Vector Core) was injected into SIn. For dual projection optogenetic experiments, 100-150 nL of AAV.2/1.syn.ChR2.EYFP (Penn Vector Core) was subsequently injected into the center of M2. For calcium imaging experiments, 500-700 nL of AAV.2/1.syn.FLEX.GCaMP6s (University of Pennsylvania Vector Core) was injected into SIn. To image the activity of $M2_{ACtx}$ axons, a total of 100 nL of AAV.2/1.syn.GCaMP6s was injected into M2 at two locations. For rabies tracing from SIn, 150-300 nL of AAV.1.CAG.FLEX.RG and AAV.1.EF1α.FLEX.TVA-mCherry was injected into SIn, and 100-200 nL of CAV-Cre (Universitat Autonoma de Barcelona, Unitat de Producció de Vectors) was subsequently injected into ACtx. Animals were allowed to recover for 14 days following injection. For rabies tracing experiments, animals underwent a second surgery, and 500-600 nL of EnVA-RΔG.GFP (Duke University Viral Vector Core) was injected into the site of TVA and RG expression (ACtx or SIn). Those mice were then allowed to survive for 7 days before perfusion.

Slice Electrophysiology and Photostimulation

Mice were deeply anesthetized with isoflurane and transcardially perfused with an ice-cold carbogenated sucrose artificial CSF (ACSF) containing the following (in mM): 2.5 KCl, 3.8 $MgCl_2$, 0.138 NaH_2PO_4, 2.2 $NaHCO_3$, 1.98 dextrose, and 81.46 sucrose. The brain was removed, and the rostral pole was glued to the stage of a vibrating microtome (Leica). 300 μm coronal slices were cut in a bath of ice-cold carbogenated sucrose ACSF. Slices were incubated for 14 min in a 34°C bath of normal ACSF (nACSF)

containing (in mM): 119 NaCl, 2.5 KCl, 1.30 $MgCl_2$, 2.5 $CaCl_2$, 1.0 NaH_2PO_4, 26.2 $NaHCO_3$, and 11.0 dextrose. Slices were then allowed to gradually reach room temperature, where they remained for the duration of the experiment. Patch electrodes (2–6 MΩ) were filled with internal solution of 5 mM QX-314, 2 mM ATP Mg salt, 0.3 mM GTP Na salt, 10 mM phosphocreatine, 0.2 mM EGTA, 2 mM $MgCl_2$, 5 mM NaCl, 10 mM HEPES, 120 mM cesium methanesulfonate, 0.15% Neurobiotin, and 0.1 mM Alexa Fluor 594 cadaverine or 0.1 mM Alexa Fluor 488 Na salt. All recordings were made using a Multiclamp 700B amplifier, the output of which was digitized at 10 kHz (Digidata 1440A). Series resistance was always < 25 MΩ and was compensated up to 90%. Pharmacological agents included 50 μM AP5 (Tocris), 20 μM NBQX (Tocris), 10 μM Gabazine (Tocris), 5 μM atropine (Sigma), 100 μM mecamylamine (Sigma), and were bath applied for > 10 min before recordings were made. Neurons were targeted using differential interference contrast and epifluorescence when appropriate. Cell morphology was visualized after intracellular dialysis with fluorescent dye. ChR2-expressing axon terminals were stimulated by 10 ms laser pulses (gated by a Uniblitz shutter) of 473 nm laser (Shanghai Laser and Optics Century Company) delivered through a fiber optic directed at the recording site. Brain slices were histologically processed to visualize Neurobiotin-filled cells using streptavidin Alexa 488, 546, or 647. For experiments represented in Supplemental Figure 4, additional measures were taken to identify pyramidal cells and different classes of interneurons. First, potassium gluconate-containing intracellular solution was substituted for solution containing cesium and QX-314, in order to make recordings in current clamp configuration and characterize intrinsic electrophysiological properties of targeted neurons (Kawaguchi. 1993,1995). Second, targeted neurons were visualized by both intracellular diffusion of fluorescent dye, as well as streptavidin-Alexa Fluor processing. Third, glutamate decarboxylase (GAD65 and GAD67) immunohistochemistry was performed to characterize the neurotransmitter phenotype of Neurobiotin-labeled cells.

In Vivo Intracellular Electrophysiology

One to 7 days before physiology, mice were anesthetized with isoflurane and a custom titanium plate was attached to the skull with Metabond (Parkell), leaving ACtx exposed. For recording from awake mice, animals were acclimated to head fixation for several days. The day of recording, mice were briefly anesthetized with isoflurane, and a small craniotomy was made over ACtx, and mice were then allowed to recover for anesthesia. For recording from anesthetized mice, animals were anesthetized with three intraperitoneal injections of 20% urethane (9.5 ml/kg) separated by 30 min. A small craniotomy was then made over ACtx. Sharp borosilicate glass electrodes were fabricated with a horizontal puller (P-97, Sutter Instruments), and tips were filled with 3M K-acetate containing 5% Neurobiotin, resulting in electrode impedances ranging from 80 to 120 MΩ. An electrode was placed in an Axoclamp headstage (HS-2A) and was lowered vertically into the brain with a hydraulic manipulator (SD Instruments) until the tip penetrated a neuron. Intracellular signals were acquired with a Power 1401 using Spike 2 (Cambridge

Electronic Design), and used for further analysis only if the resting membrane potential was less than -50 mV and was modulated by an auditory stimulus.

In Vivo Extracellular Electrophysiology

Preparatory surgical procedures and stimulus presentation were the same as for intracellular recordings in anesthetized head-fixed mice. One day before recording, a large craniotomy was made over ACtx, which was then covered with silicone elastomer (Kwik-Sil). On recording day, a 32-channel (4 x 8; 0.8 x 0.8 mm recording area) multielectrode array (NeuroNexus) was lowered vertically into ACtx and allowed to rest for 30 min. The electrode array was connected directly to a digitizing headstage (Intan Technologies) via a 36-pin connector (Omnetics). Neural activity was referenced to an AgCl pellet implanted over contralateral somatosensory cortex. Voltage traces were filtered (300 to 5,000 Hz), digitized, and recorded (20 kHz per channel) for offline analysis. Putative action potentials were identified by voltage events crossing a threshold and individual neurons were sorted based on spike features using custom software.

2 Photon Calcium Imaging

Three to four weeks following the GCaMP6s injection, mice were anaesthetized with isoflurane and a custom, Y-shaped titanium plate was attached to the skull with Metabond. Mice were acclimated to head fixation for 1–5 days before the initial imaging session, and 30 µL dexamethasone (4 mg/ml) was administered (intramuscularly) on the last acclimation day, 6–12 h before windowing. A rectangular craniotomy was then made over the injection site, and a laminated glass coverslip was placed over the craniotomy and sealed with Metabond. Animals were allowed to recover for 24 hours. Imaging was performed using a resonant scanning two-photon microscope (Neurolabware) with a mode-locked titanium sapphire laser (Mai Tai DeepSee) at 920 nm. Images were acquired at 15.5 Hz with a 16x 0.8 NA water-immersion objective (Nikon). Imaging was performed in low light conditions, with illumination only from an infrared light source. The mouse was free to move or rest on a non-motorized movable disc, rotations of which were monitored using a rotary encoder (U.S. Digital). A small infrared-sensitive video camera (Logitech) was positioned to monitor body movements. A GigE Vision camera (Dalsa) was used to monitor changes in pupil size at an acquisition rate synchronized to that of the microscope. GCaMP fluorescence images were registered to correct for movement artifact in the horizontal plane. Regions of interest (ROIs) were selected either by manually tracing around short, independent segments of axon, or by using semi-automated identification of nearby correlated pixel activity (Scanbox). For imaging SIn_{ACh} axons, ΔF/F was calculated using the mean fluorescence signal from 1-2 min of data acquisition as baseline. For imaging $M2_{ACtx}$ axons, ΔF/F was calculated using a baseline value of the 30^{th} percentile of fluorescence of each ROI (Petreanu et al., 2012).

Movement and Pupil Size Tracking

Video of body movements and acquired 2p images were synchronized post hoc using an aperiodic train of digital pulses that was simultaneously sent to the camera and microscope. Body movements were detected offline using ROIs drawn around the head (including mouth, nose, and whiskers), forelimbs, and treadmill perimeter, as well as a red LED used to synchronize video and 2p data. Within each ROI, the average change in pixel intensity was calculated across video frames as a measure of movement. Pupil size was similarly quantified by measuring the change in average pixel intensity within an ROI drawn around the eye. Because there was substantial reflected and emitted infrared light, the pupil was easily visualized, with increases in pupil size corresponding to increased brightness within the eye ROI. Pupil area traces were low-pass filtered to remove movement artifacts, which were clearly distinguishable from both slow and fast pupil dilations and constrictions.

Histology and Confocal Microscopy

Mice were deeply anaesthetized with sodium pentobarbital (250 mg/kg, intraperitoneally) and transcardially perfused with phosphate buffered saline (PBS) followed by 4% cold paraformaldehyde. Brains were post-fixed overnight in 4% paraformaldehyde containing 30% sucrose. Brains were blocked in Optimum Cutting Temperature compound (Tissue-Tek), and 50 µm coronal sections were cut on a sliding freezing microtome. Brain slices were first rinsed in PBS for 10 min, then in two washes of PBS containing 0.3% Triton X-100 (PBST) for 20 min. Slices were then incubated in PBST with 10% Blocking One blocking buffer (Nacalai Tesque) for 1 h at room temperature. Immunostaining was performed with primary antibodies of rabbit anti-GFP (1:1,000; Abcam), goat anti-ChAT (1:1000; Millipore), mouse anti-PV (1:1,000; Swant), mouse anti-NeuN (1:100; Millipore), rabbit anti-VIP (1:1000; Immunostar), rabbit anti-NPY (1:1000; Abcam), rabbit anti-5HT (1:1000; Millipore), rabbit anti-DBH (1:1000; Millipore), rabbit anti-GAD65/67 (1:1,000; Abcam), or rabbit anti-SST (1:1000; Santa Cruz) for 2-3 nights at 4°C. After three washes of 10 min in PBS, slices were incubated in secondary antibodies from Jackson Immunoresearch at a concentration of 1:1000 in PBST containing 10% blocking buffer overnight at 4°C. To label nicotinic acetylcholine receptors in a subset of experiments, α-bungarotoxin conjugated to Alexa Fluor 647 (1:1000, Molecular Probes) was included. Sections were washed several times in PBS, incubated in PBS containing DAPI for 30 min for a subset of experiments, rinsed again, and mounted. For visualizing Neurobiotin cell fills, permeabilized 75 µm sections were incubated overnight in PBST containing streptavidin Alexa 546, 488, or 647. Images were acquired with a Zeiss 710 LSM inverted confocal microscope using 10x, 20x, 60x oil immersion, or 100x oil immersion objectives. For high magnification imaging of axons, optical sections of 1 or fewer Airy units using a 100x 1.4 NA objective were acquired. All image processing was performed in ImageJ. For presentation, some images were median filtered with a window radius of one pixel. Additionally, a subset of Z stacks underwent 3D interpolation with a resampling factor of one (3D Viewer, Image J) to permit rotated views of images.

Data Analysis

All data analyses were performed in Matlab. For all statistical tests, significance was measured against an alpha of 0.05. To calculate the relative location of SIn cell bodies in rabies-based presynaptic labeling experiments, the mediolateral and dorsoventral coordinates of each neuron from two brains for each genotype were measured relative to the midline near fasciola cinerea, or the most medial point of CA1 of hippocampus. The rostrocaudal location of each brain section was indexed by measuring the mediolateral length of hippocampus, which progressively increased for caudal sections. Then, the coordinates were normalized to the width and height of each section to account for variability in brain size. For brain slice electrophysiology, peak current was measured from an average of 4 or 8 stimulus trials within a response window of 2 seconds after stimulus onset. Conservative estimates of onset times for excitatory and inhibitory currents were calculated by finding the times at which those currents deviated from 2.5 times the standard deviation of the pre-stimulus baseline period. For in vivo intracellular experiments, voltage area evoked for each neuron was calculated for each of 20 (light stimulus or blank stimulus alone) or 40 (tone + light stimulus) trials within a 2 second window after stimulus onset. For multielectrode data, individual unit responses were included for analysis if they were significantly driven by stimulus presentation in both laser off and laser on conditions. Response strength (RS), in units of spikes/s, was calculated from a 100 ms window after tone onset relative to a 200 ms baseline period before any stimulus presentation. Peristimulus time histograms were calculated by smoothing the action potential firing rate over a 20 ms window. Population tuning curves were created by normalizing the tone response of each isolated unit to its peak response. Those same normalization criteria were then applied to those units' responses to tone presentation with concurrent light presentation. The tuning curves of each normalized, isolated unit were then aligned to produce a peak of 1 at the preferred tone frequency. Normalized response strength for each tone (± 0, 1, 2, and 3 octaves relative to the preferred frequency) were plotted against the normalized response strength for each tone with light presentation, and a line was fit to these data points. To calculate time constants for currents evoked in dual optogenetic experiments, exponentials were fit to the onset and offset of each of 5 neurons' evoked excitatory current before and after application of receptor blockers. Tau_{On} was calculated by fitting an exponential from baseline to the peak evoked current. Tau_{Off} was calculated by fitting an exponential from peak evoked current back to baseline. For calcium imaging experiments, periods of movement were identified by setting a threshold for each body ROI and treadmill ROI. Mean fluorescence was then calculated for 500 ms windows 1 s before and 1 s after movement onset. To calculate lags between movement and pupil or axon fluorescence traces, the peak cross correlation coefficients within a ± 2 s window were calculated and averaged across multiple ROIs and movement epochs from several mice. Mean axon fluorescence and pupil size were aligned to both movement onset and movement offset.

Supplemental References

Kawaguchi, Y. (1993). Groupings of Nonpyramidal and Pyramidal Cells with Specific Physiological and Morphological-Characteristics in Rat Frontal-Cortex. Journal of neurophysiology 69, 416-431.

Kawaguchi, Y. (1995). Physiological Subgroups of Nonpyramidal Cells with Specific Morphological-Characteristics in Layer Ii/Iii of Rat Frontal-Cortex. J Neurosci 15, 2638-2655.

Petreanu, L., Gutnisky, D.A., Huber, D., Xu, N.L., O'Connor, D.H., Tian, L., Looger, L., and Svoboda, K. (2012). Activity in motor-sensory projections reveals distributed coding in somatosensation. Nature 489, 299-303.

Unal, C.T., Golowasch, J.P., and Zaborszky, L. (2012). Adult mouse basal forebrain harbors two distinct cholinergic populations defined by their electrophysiology. Frontiers in Behavioral Neuroscience *6*, 21.